

Hydrothermal Syntheses, Structures, and Properties of Three 3-D Lanthanide Coordination Polymers that Form 1-D Channels

Xiang-Jun Zheng,^[a] Zhe-Ming Wang,^[b] Song Gao,^[b] Fu-Hui Liao,^[b] Chun-Hua Yan,^[b] and Lin-Pei Jin*^[a]

Keywords: Coordination polymer / Hydrothermal synthesis / Lanthanides / 2,6-Naphthalenedicarboxylate / X-ray diffraction

We report the hydrothermal synthesis and crystal structure of isostructural lanthanide coordination polymers $[\text{Ln}_2(\text{NDC})_3(\text{phen})_2] \cdot \text{H}_2\text{NDC}$ [$\text{Ln} = \text{Tb}$ (**1**), Ho (**2**) and Yb (**3**)] that feature 2,6-naphthalenedicarboxylate (NDC) and 1,10-phenanthroline (phen) ligands. The NDC ligands bridge the lanthanide ions in two different modes to form a 3-D porous framework that accommodates large, neutral 2,6-naphthalenedicarboxylic acid molecules as guests in the channels, stabilized through O–H...O hydrogen bonds to the NDC li-

gand. The effective dimension of the channel is ca. 6.0×8.2 Å. Thermogravimetric analysis shows that complex **2** remains stable up to 330 °C, which we confirmed also by powder X-ray diffraction analyses. The framework collapsed upon the loss of the coordinating phen molecules. The Tb complex shows strong evidence of ferromagnetic coupling interactions.

(© Wiley-VCH Verlag GmbH & Co. KGaA, 69451 Weinheim, Germany, 2004)

Introduction

The synthesis of coordination polymers remains a subject of intense interest. Accordingly, a large number of coordination polymers of different dimensions and various topologies have been reported.^[1–19] Recent research in this field has focused on producing materials designed to perform highly specific and cooperative functions.^[20–25] Advances in the design and synthesis of metal-organic frameworks (MOFs) has led to numerous practical and conceptual developments in that direction.^[26–30] Specifically, the chemistry of MOFs provides an extensive array of crystalline materials that have high stability, tunable metrics, organic functionalities, and porosity.^[31] The wide variety of possible organic linkers and the multiple physical properties of inorganic metal ions make it feasible to modulate both the dimensions of the pores and the properties of the final porous coordination polymers. In such structures, organic species act as either pillars or linkers to arrange inorganic layers, chains, or clusters of transition or lanthanide ions.^[32] Polycarboxylic acids are frequently utilized to construct microporous compounds.^[33–36] In the study of lanthanide-organic frameworks, rigid polycarboxylic acids, especially dicarboxylic acids, are frequently used to link lanthanide

ions^[17,37] or lanthanide cubane-like clusters.^[38,39] Considering the high coordination numbers of lanthanide ions, ancillary ligands also can be incorporated into the lanthanide coordination networks. Bulky ancillary ligands can occupy some coordination sites and reduce the interpenetration of frameworks, which results in an increase in the dimensions of the pores in the framework. 2,6-Naphthalenedicarboxylate is a rigid linear ligand whose transition metal coordination polymers, both binary and ternary, have been studied extensively,^[40–46] but only three binary coordination polymers of its lanthanide analogues have been reported.^[47–49] No ternary lanthanide coordination polymers of 2,6-naphthalenedicarboxylate have been described in the literature. In this study, we selected 2,6-naphthalenedicarboxylate as the linker and a chelating ligand, 1,10-phenanthroline, as the ancillary ligand to construct a ternary lanthanide-organic framework that is thermally stable and exhibits interesting magnetic behavior.

Results and Discussion

Synthetic Considerations

Dipotassium 2,6-naphthalenedicarboxylate readily forms a precipitate upon the addition of lanthanide chlorides. Therefore, for the preparation of our coordination polymers, first we acidified dipotassium 2,6-naphthalenedicarboxylate to prevent it from reacting too quickly with the lanthanide chloride; this process facilitates coordination of phen molecules and leads to the growth of crystals of the ternary complex. In this approach, some phen molecules

^[a] Department of Chemistry, Beijing Normal University, Beijing 100875, P. R. China
Fax: (internat.) + 86-1062202075
E-mail: lpjin@bnu.edu.cn

^[b] State Key Laboratory of Rare Earth Materials Chemistry and Applications, College of Chemistry and Molecular Engineering, Peking University, Beijing, 100871, P. R. China

act as ligands to coordinate with lanthanide ions, while others act as mild organic bases that deprotonate H_2NDC units to give NDC ions that then coordinate with lanthanide ions.

Crystal Structures

The three complexes are isomorphous and isostructural; we describe in detail only the structure of complex **2**. The asymmetric unit of **2** consists of one Ho^{III} center, 1.5 NDC anions, one phen ligand, and 0.5 H_2NDC guest units. Around the central metal ion, there is a bidentate chelating phen ligand and four bridging NDC anions (Figure 1). The Ho^{III} ion is eight-coordinate with two ligating nitrogen atoms from a phen molecule and six oxygen atoms from four NDC anions; this arrangement results in a triangular dodecahedral coordination polyhedron. For convenience, the NDC anions having the oxygen atoms labeled O1, O3, and O5 (Figure 1) are named NDC1, NDC2, and NDC3, respectively. These structures represent the three orientations of NDC anions in the crystal; the dihedral angles between the naphthalene rings of NDC1 and NDC2, NDC2 and NDC3, and NDC1 and NDC3 are 108.2, 68.0, and 94.7 °C, respectively. In the title coordination polymers, the NDC anions adopt two coordination modes: bis(bridging bidentate) (I) and bis(chelating bidentate) (II), as depicted in Scheme 1. NDC1 ligands adopt the type I binding mode, whereas NDC2 and NDC3 ligands adopt type II binding.

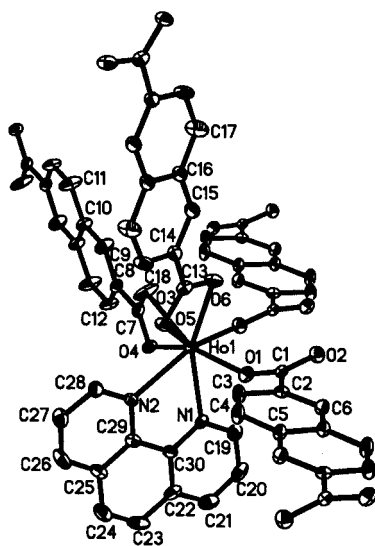
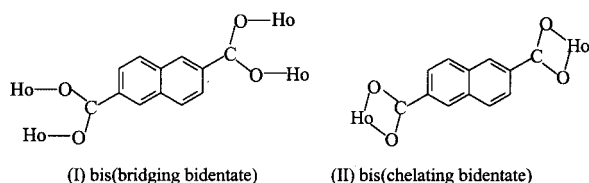


Figure 1. Coordination environment of complex **2**; the asymmetric unit and the related coordination atoms are labeled; guest molecules and all hydrogen atoms have been omitted for clarity; thermal ellipsoids are drawn at 30% probability



Scheme 1. Coordination modes of the NDC ligand in complex **2**

The framework structure of **2** is built from a dinuclear unit, $\text{Ho}_2(\text{NDC})_3(\text{phen})_2$, which results from the linking of two asymmetric units through two carboxylate units of two NDC1 anions. First, the NDC1 ligands link the dinuclear building units to form 1-D chains along the c -axis (Figure 2). The distance between the adjacent dinuclear units in the chain is 12.25 Å. Next, the NDC2 ligands link two Ho^{III} ions ($\text{Ho}\cdots\text{Ho}$, 13.34 Å), in the $[01\bar{1}]$ direction, of two adjacent chains to form 2-D layers that feature 44-membered

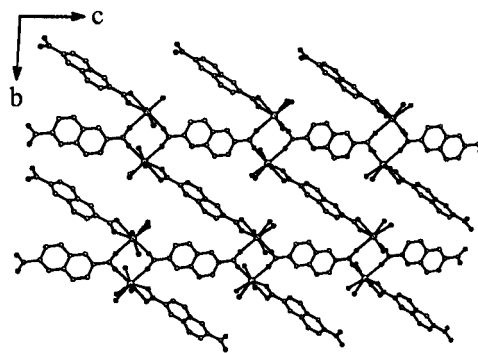


Figure 2. 2-D layers, viewed along the a -axis, featuring 44-membered ring channels constructed with Ho^{III} , NDC1, and NDC2 ligands

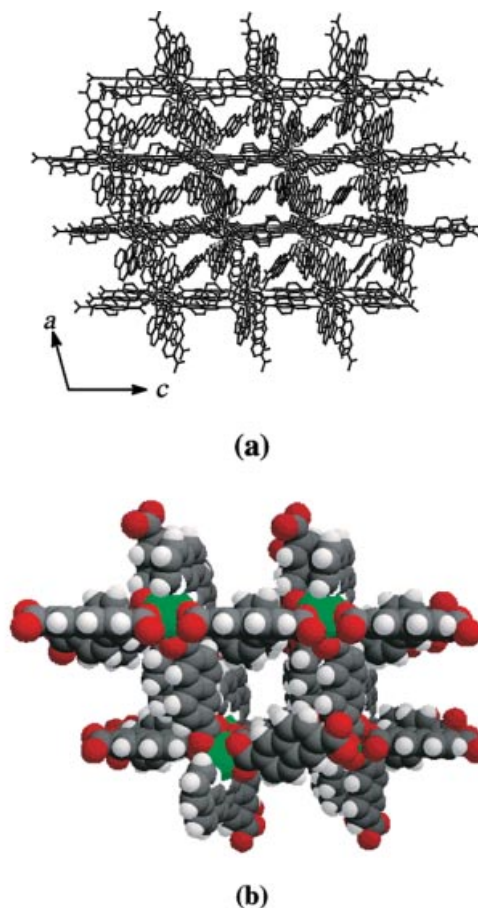


Figure 3. (a) 3-D porous framework of complex **2**, viewed along the b -axis, showing the guest molecules accommodated in the 1-D channels; all hydrogen atoms have been omitted for clarity; (b) space-filling model of complex **2** showing the 1-D channel; the guest molecules have been omitted for clarity

parallelogram channels (Figure 2). Finally, the NDC3 ligands, which act as pillars, link the Ho^{III} ions (Ho^{III}...Ho, 13.35 Å), in the [110] direction, from two adjacent layers to form the porous 3-D framework (Figure 3).

When viewed along the *b*-axis, complex **2** exhibits many 1-D channels. Despite the large dimensions of the cross-section of the channel (internuclear separation: 13.34×13.35 Å) arising from the long span of the NDC ligand (ca. 9.0 Å), the effective dimension of the channel is only 6.0×8.2 Å (van der Waals free space) because of the presence of the bulky phen molecules in the channel. The large neutral guest molecules (H₂NDC), which are hydrogen bonded to the coordinating oxygen atoms of the NDC3 ligands in the

framework, are accommodated within the channels. The two carboxyl groups of the guest molecule are arrayed in the diagonal direction of the parallelogram channel. The geometries of the hydrogen bonds in complexes **1**, **2**, and **3** are listed in Table 1. Selected bond lengths within **1**, **2**, and **3** are listed in Table 2.

Analysis of the Thermal Stability of **2**

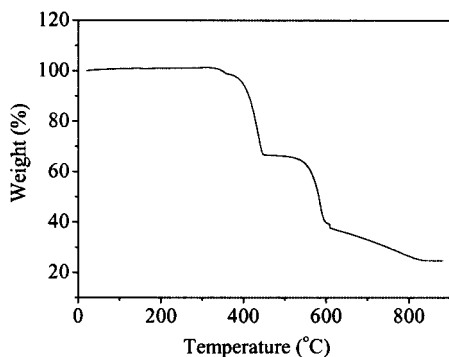
The existence of guest molecules in the channels inspired us to investigate the thermal stability of the coordination polymers; we took complex **2** as a representative example to carry out the TG analysis. We observe from the thermogravimetric curve of **2** (Figure 4) that this complex remains stable up to 330 °C, at which temperature the first weight loss occurred, i.e., loss of the H₂NDC guest molecule. A second weight loss occurred when the temperature reached 357 °C. The H₂NDC guest molecule was not completely removed before the loss of two coordinating phen molecules occurred. One H₂NDC guest molecule and two coordinating phen molecules were completely removed at 460 °C; this process occurs with a weight loss of 35.2% (calculated: 37.2%). The decomposition of the complex continued at

Table 1. The geometries of hydrogen bonds in complexes **1**, **2**, and **3** [Å; °] (symmetry operations: ^{#1} $-x, -y, -z$; ^{#2} $-x, -y + 1, -z$)

| Complex | D–H...A | <i>d</i> (D–H) | <i>d</i> (H...A) | <i>d</i> (D...A) | <(DHA) |
|----------|--------------------------|----------------|------------------|------------------|--------|
| 1 | O7–H7...O4 ^{#1} | 0.820 | 1.870 | 2.637 | 156.0 |
| 2 | O7–H7...O6 ^{#2} | 0.820 | 1.978 | 2.660 | 140.11 |
| 3 | O7–H7...O4 ^{#1} | 0.820 | 1.810 | 2.660 | 179.9 |

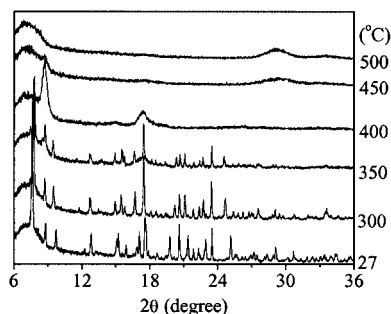
Table 2. Selected bond lengths [Å] and bond angles [°] for complexes **1**, **2**, and **3** (symmetry operations: ^{#1} $-x, -y, -z$; ^{#2} $-x, -y + 2, -z$)

| 1 | | 2 | | 3 | |
|--------------------------------|------------|--------------------------------|------------|--------------------------------|------------|
| Tb(1)–O(1) | 2.454(3) | Ho(1)–O(1) | 2.227(5) | Yb(1)–O(1) | 2.465(3) |
| Tb(1)–O(2) | 2.383(3) | Ho(1)–O(2) ^{#2} | 2.238(5) | Yb(1)–O(2) | 2.374(4) |
| Tb(1)–O(3) | 2.391(3) | Ho(1)–O(3) | 2.336(5) | Yb(1)–O(3) | 2.388(3) |
| Tb(1)–O(4) | 2.476(3) | Ho(1)–O(4) | 2.437(5) | Yb(1)–O(4) | 2.475(3) |
| Tb(1)–O(5) | 2.262(3) | Ho(1)–O(5) | 2.356(5) | Yb(1)–O(5) | 2.261(3) |
| Tb(1)–O(6) ^{#1} | 2.272(3) | Ho(1)–O(6) | 2.439(5) | Yb(1)–O(6) ^{#1} | 2.271(3) |
| Tb(1)–N(1) | 2.535(3) | Ho(1)–N(1) | 2.496(6) | Yb(1)–N(1) | 2.539(4) |
| Tb(1)–N(2) | 2.524(3) | Ho(1)–N(2) | 2.496(5) | Yb(1)–N(2) | 2.539(4) |
| O(5)–Tb(1)–O(6) ^{#1} | 89.54(10) | O(1)–Ho(1)–O(2) ^{#2} | 89.45(18) | O(5)–Yb(1)–O(6) ^{#1} | 89.60(12) |
| O(5)–Tb(1)–O(2) | 153.10(11) | O(1)–Ho(1)–O(3) | 152.56(19) | O(5)–Yb(1)–O(2) | 152.71(14) |
| O(6) ^{#1} –Tb(1)–O(2) | 90.35(11) | O(2) ^{#2} –Ho(1)–O(3) | 88.7(2) | O(6) ^{#1} –Yb(1)–O(2) | 89.11(15) |
| O(5)–Tb(1)–O(3) | 81.26(10) | O(1)–Ho(1)–O(5) | 82.06(18) | O(5)–Yb(1)–O(3) | 81.71(12) |
| O(6) ^{#1} –Tb(1)–O(3) | 138.04(9) | O(2) ^{#2} –Ho(1)–O(5) | 138.61(17) | O(6) ^{#1} –Yb(1)–O(3) | 138.28(12) |
| O(2)–Tb(1)–O(3) | 80.93(10) | O(3)–Ho(1)–O(5) | 81.36(18) | O(2)–Yb(1)–O(3) | 81.22(13) |
| O(5)–Tb(1)–O(1) | 151.44(10) | O(1)–Ho(1)–O(4) | 151.49(17) | O(5)–Yb(1)–O(1) | 151.72(12) |
| O(6) ^{#1} –Tb(1)–O(1) | 77.96(9) | O(2) ^{#2} –Ho(1)–O(4) | 78.55(17) | O(6) ^{#1} –Yb(1)–O(1) | 78.45(12) |
| O(2)–Tb(1)–O(1) | 53.81(9) | O(3)–Ho(1)–O(4) | 53.94(17) | O(2)–Yb(1)–O(1) | 53.72(12) |
| O(3)–Tb(1)–O(1) | 124.84(9) | O(5)–Ho(1)–O(4) | 123.67(16) | O(3)–Yb(1)–O(1) | 123.90(12) |
| O(5)–Tb(1)–O(4) | 79.32(10) | O(1)–Ho(1)–O(6) | 79.29(17) | O(5)–Yb(1)–O(4) | 79.36(13) |
| O(6) ^{#1} –Tb(1)–O(4) | 84.48(9) | O(2) ^{#2} –Ho(1)–O(6) | 84.29(17) | O(6) ^{#1} –Yb(1)–O(4) | 84.81(12) |
| O(2)–Tb(1)–O(4) | 73.89(10) | O(3)–Ho(1)–O(6) | 73.28(18) | O(2)–Yb(1)–O(4) | 73.37(14) |
| O(3)–Tb(1)–O(4) | 53.62(9) | O(5)–Ho(1)–O(6) | 54.35(16) | O(3)–Yb(1)–O(4) | 53.50(11) |
| O(1)–Tb(1)–O(4) | 124.03(9) | O(4)–Ho(1)–O(6) | 124.31(16) | O(1)–Yb(1)–O(4) | 124.18(12) |
| O(5)–Tb(1)–N(2) | 99.89(10) | O(1)–Ho(1)–N(1) | 76.39(18) | O(5)–Yb(1)–N(1) | 76.27(12) |
| O(6) ^{#1} –Tb(1)–N(2) | 148.72(10) | O(2) ^{#2} –Ho(1)–N(1) | 87.82(19) | O(6) ^{#1} –Yb(1)–N(1) | 88.04(13) |
| O(2)–Tb(1)–N(2) | 94.05(12) | O(3)–Ho(1)–N(1) | 130.86(19) | O(2)–Yb(1)–N(1) | 130.92(13) |
| O(3)–Tb(1)–N(2) | 73.16(10) | O(5)–Ho(1)–N(1) | 128.38(19) | O(3)–Yb(1)–N(1) | 128.30(12) |
| O(1)–Tb(1)–N(2) | 79.81(10) | O(4)–Ho(1)–N(1) | 77.38(17) | O(1)–Yb(1)–N(1) | 77.77(12) |
| O(4)–Tb(1)–N(2) | 126.45(9) | O(6)–Ho(1)–N(1) | 154.47(17) | O(4)–Yb(1)–N(1) | 154.62(13) |
| O(5)–Tb(1)–N(1) | 76.14(10) | O(1)–Ho(1)–N(2) | 99.71(18) | O(5)–Yb(1)–N(2) | 99.21(13) |
| O(6) ^{#1} –Tb(1)–N(1) | 88.65(10) | O(2) ^{#2} –Ho(1)–N(2) | 148.46(19) | O(6) ^{#1} –Yb(1)–N(2) | 148.39(12) |
| O(2)–Tb(1)–N(1) | 130.75(11) | O(3)–Ho(1)–N(2) | 96.1(2) | O(2)–Yb(1)–N(2) | 96.07(16) |
| O(3)–Tb(1)–N(1) | 127.61(10) | O(5)–Ho(1)–N(2) | 72.85(18) | O(3)–Yb(1)–N(2) | 73.28(12) |
| O(1)–Tb(1)–N(1) | 77.97(9) | O(4)–Ho(1)–N(2) | 79.26(18) | O(1)–Yb(1)–N(2) | 79.68(12) |
| O(4)–Tb(1)–N(1) | 154.55(11) | O(6)–Ho(1)–N(2) | 126.96(18) | O(4)–Yb(1)–N(2) | 126.56(11) |
| N(2)–Tb(1)–N(1) | 65.27(10) | N(1)–Ho(1)–N(2) | 65.58(19) | N(1)–Yb(1)–N(2) | 65.12(13) |

Figure 4. Thermogravimetric curve of complex **2**

491 °C and ended at 840 °C, at which point a residue, Ho_2O_3 , was obtained in 24.8% yield (calculated: 24.4%).

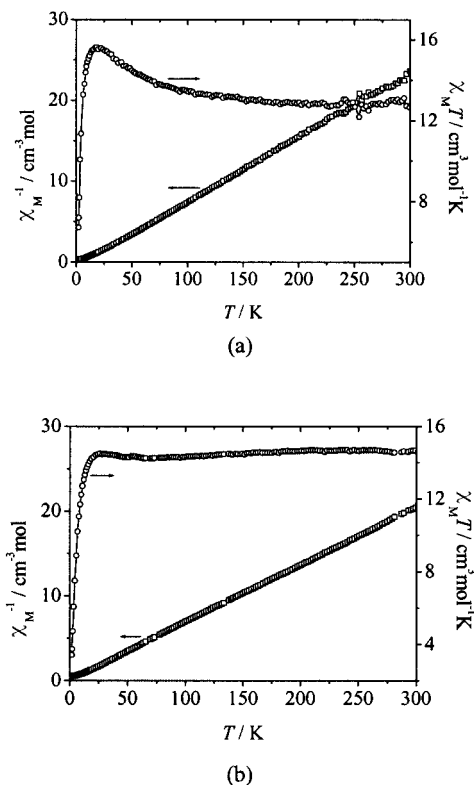
To further test the thermal stability of **2**, we examined powder samples by variable-temperature X-ray diffraction analysis. The powder XRD patterns of **2** (Figure 5) at 27, 300, 350, 400, and 500 °C were recorded. We see in Figure 5 that when the temperature rose from 27 to 300 °C, the positions of the major peaks undergo no significant changes, but some peaks shift slightly to lower or higher 2θ values. This observation indicates that a possible distortion of the structure had occurred, but it did not affect the existence of the framework. The similarities between the powder XRD patterns obtained at 300 and 350 °C also suggest that the framework remains stable at 350 °C, i.e., when phen molecules are still present, which is in accordance with the results of the thermogravimetric analysis. Above 400 °C, however, the PXRD patterns are changed completely, which indicates that a collapse of the framework has occurred. The loss of the coordinating phen molecules may account for the framework's collapse, i.e., the presence of the coordinating phen molecules is required for a stable framework.

Figure 5. Powder X-ray diffraction patterns of **2** at different temperatures [the large broad peak at $< 10^\circ$ (2θ) arose from the use of the position scan detector]

Because of similarities between the frameworks of the title complexes, we deduced that **1** and **3** have stabilities similar to that of **2**.

Magnetic Properties

We investigated the magnetic properties of complexes **1** and **2** in the solid state at 1 T within the temperature range 2–300 K (Figure 6).

Figure 6. Plots of the temperature dependences of χ_M^{-1} (open squares) and $\chi_M T$ (open circles) for complexes **1** (a) and **2** (b)

For **1**, the observed value of $\chi_M T$ per [Tb] unit is $12.82 \text{ cm}^3 \cdot \text{K} \cdot \text{mol}^{-1}$ at room temperature (Figure 6a), which is slightly larger than the value expected for a free Tb^{3+} ion ($11.82 \text{ cm}^3 \cdot \text{K} \cdot \text{mol}^{-1}$).^[50] Upon cooling, the value of $\chi_M T$ increases up to a maximum of $15.62 \text{ cm}^3 \cdot \text{K} \cdot \text{mol}^{-1}$ at ca. 18 K. The plot of χ_M^{-1} vs. T over the temperature range 30–300 K obeys the Curie–Weiss law [$\chi = C/(T - \theta)$] with $C = 12.5 \text{ cm}^3 \cdot \text{K} \cdot \text{mol}^{-1}$ and $\theta = 6.5 \text{ K}$. All of these results indicate that there is ferromagnetic coupling between the Tb^{3+} ions. The value of $\chi_M T$ decreases abruptly at temperatures below 18 K to reach $6.70 \text{ cm}^3 \cdot \text{K} \cdot \text{mol}^{-1}$ at 2 K. This feature is due primarily to the splitting of the ligand field of the Tb^{3+} ion as a result of strong spin-orbital coupling. For **2**, the observed value of $\chi_M T$ per [Ho] unit is $14.65 \text{ cm}^3 \cdot \text{K} \cdot \text{mol}^{-1}$ at room temperature (Figure 6b), which is close to the value expected ($14.07 \text{ cm}^3 \cdot \text{K} \cdot \text{mol}^{-1}$) for a free Ho^{3+} ion.^[50] The value of $\chi_M T$ decreases slowly as the temperature decreases to ca. 26 K ($14.48 \text{ cm}^3 \cdot \text{K} \cdot \text{mol}^{-1}$) and then it drops rapidly below 26 K to reach a value of $3.40 \text{ cm}^3 \cdot \text{K} \cdot \text{mol}^{-1}$ at 2 K. The plot of χ_M^{-1} vs. T over the temperature range 30–300 K obeys the Curie–Weiss law with $C = 14.76 \text{ cm}^3 \cdot \text{K} \cdot \text{mol}^{-1}$ and $\theta = -2.21 \text{ K}$. The decrease of $\chi_M T$ and the negative value of θ are due primarily to splitting of the ligand field of the Ho^{3+} ion as a result of strong spin-orbital coupling, and is attributed partly to the poss-

Table 3. Crystal data for complexes **1**, **2**, and **3**

| | 1 | 2 | 3 |
|--|--|---|--|
| Empirical formula | C ₃₆ H ₂₁ N ₂ O ₈ Tb | C ₃₆ H ₂₁ HoN ₂ O ₈ | C ₃₆ H ₂₁ N ₂ O ₈ Yb |
| Formula mass | 768.47 | 774.48 | 782.59 |
| Temperature [K] | 293(2) | 293(2) | 293(2) |
| Wavelength [Å] | 0.71073 | 0.71073 | 0.71073 |
| Crystal system | triclinic | triclinic | triclinic |
| Space group | <i>P</i> $\bar{1}$ | <i>P</i> $\bar{1}$ | <i>P</i> $\bar{1}$ |
| <i>a</i> [Å] | 10.7822(2) | 10.802(6) | 10.8762(2) |
| <i>b</i> [Å] | 12.1806(3) | 12.143(6) | 12.2294(3) |
| <i>c</i> [Å] | 12.3369(3) | 12.245(7) | 12.3328(3) |
| α [°] | 94.2028(9) | 94.031(11) | 93.9317(11) |
| β [°] | 106.3049(9) | 106.641(9) | 106.6736(11) |
| γ [°] | 100.9193(12) | 101.356(9) | 101.2612(13) |
| <i>V</i> [Å ³] | 1513.12(6) | 1495.0(14) | 1527.54(6) |
| <i>Z</i> | 2 | 2 | 2 |
| <i>D</i> _{calcd.} [g·cm ⁻³] | 1.687 | 1.720 | 1.701 |
| μ [mm ⁻¹] | 2.396 | 2.706 | 3.120 |
| Reflections collected, unique, <i>R</i> _{int} | 28830, 6894, 0.0759 | 6266, 5260, 0.0440 | 28225, 6857, 0.0684 |
| <i>R</i> indices [<i>I</i> > 2 σ (<i>I</i>)] | <i>R</i> ₁ = 0.0377, <i>wR</i> ₂ = 0.0830 | <i>R</i> ₁ = 0.0492, <i>wR</i> ₂ = 0.0846 | <i>R</i> ₁ = 0.0415, <i>wR</i> ₂ = 0.0968 |
| <i>R</i> indices (all data) | <i>R</i> ₁ = 0.0517, <i>wR</i> ₂ = 0.0883 | <i>R</i> ₁ = 0.0806, <i>wR</i> ₂ = 0.0949 | <i>R</i> ₁ = 0.0601, <i>wR</i> ₂ = 0.1032 |

ibly weak antiferromagnetic coupling between the Ho³⁺ ions in **2**.

Conclusion

We have synthesized novel 3-D porous lanthanide coordination polymers, [Ln₂(NDC)₃(phen)₂] \cdot H₂NDC (Ln = Tb, Ho, and Yb), incorporating 2,6-naphthalenedicarboxylate and 1,10-phenanthroline units by hydrothermal reactions; we characterized the complexes by single-crystal X-ray diffraction analysis. The results show that the three complexes are isostructural and that the NDC²⁻ unit is a good spacer for the construction of porous lanthanide coordination polymers. Large, neutral guest molecules (2,6-naphthalenedicarboxylic acid units) are accommodated within the 1-D channels, which are rarely found in lanthanide coordination polymers. These lanthanide coordination polymers remain thermally stable up to ca. 330 °C.

Experimental Section

General Remarks: TbCl₃·6H₂O, HoCl₃·6H₂O, and YbCl₃·6H₂O were each prepared by dissolving their respective oxides in concentrated hydrochloric acid and then evaporating the solvent to dryness. All the other reagents were commercially available and were used without further purification.

Instrumentation: Elemental analyses were obtained with an Elementar Vario EL analyzer. IR spectra were recorded with a Nicolet Avatar 360 FT-IR spectrometer by using the KBr pellet technique. Thermogravimetric analyses were performed with a TGA 951 thermogravimetric analyzer. The magnetic susceptibilities were obtained on crystal samples by using an Oxford MagLab System 2000 magnetometer. The experimental susceptibilities were corrected for the presence of the sample holder and the diamagnetism contributions were estimated from Pascal's constants. The powder X-ray diffraction patterns were recorded using a Bruker AXS D8 ADVANCE diffractometer.

[Tb₂(NDC)₃(phen)₂] \cdot H₂NDC (1**):** Hydrochloric acid (1.65 mol·L⁻¹, 4 drops) was added with stirring to a mixture of dipotassium 2,6-naphthalenedicarboxylate (0.044 g, 0.15 mmol) and H₂O (10 mL). TbCl₃·6H₂O (0.038 g, 0.1 mmol) and phen·H₂O (0.04 g, 0.2 mmol) were then added. The mixture was sealed in a 25-mL stainless steel reactor equipped with a Teflon liner and heated at 170 °C for 72 h. Light-yellow crystals of **1** were obtained (0.015 g, 26.0%). C₃₆H₂₁N₂O₈Tb (768.47): calcd. C 56.27, H 2.75, N 3.65; found C 55.98, H 2.53, N 3.55. IR (KBr pellet): $\tilde{\nu}$ = 3433 m, 1705 m, 1617 m, 1548 m, 1493 m, 1422 s, 1362 m, 805 m, 792 m, 727 m cm⁻¹.

[Ho₂(NDC)₃(phen)₂] \cdot H₂NDC (2**):** The same procedure was applied as that for **1**, but with the following quantities: dipotassium 2,6-naphthalenedicarboxylate (0.044 g, 0.15 mmol), H₂O (10 mL), hydrochloric acid (1.65 mol·L⁻¹, 4 drops), HoCl₃·6H₂O (0.038 g, 0.1 mmol), and phen·H₂O (0.04 g, 0.2 mmol). Light-yellow crystals of **2** were obtained (0.018 g, 31.0%). C₃₆H₂₁HoN₂O₈ (774.48): calcd. C 55.83, H 2.73, N 3.62; found C 55.56, H 2.37, N 3.54. IR (KBr pellet): $\tilde{\nu}$ = 3439 m, 1705 m, 1619 m, 1552 m, 1494 m, 1423 s, 1362 m, 806 m, 792 m cm⁻¹.

[Yb₂(NDC)₃(phen)₂] \cdot H₂NDC (3**):** The same procedure was applied as that for **1**, but with the following quantities: dipotassium 2,6-naphthalenedicarboxylate (0.044 g, 0.15 mmol), H₂O (10 mL), hydrochloric acid (1.65 mol·L⁻¹, 4 drops), YbCl₃·6H₂O (0.039 g, 0.1 mmol), and phen·H₂O (0.04 g, 0.2 mmol). Light-yellow crystals of **3** were obtained (0.016 g, 27.3%). C₃₆H₂₁N₂O₈Yb (782.59): calcd. C 55.25, H 2.70, N 3.58; found C 55.63, H 2.91, N 3.72. IR (KBr pellet): $\tilde{\nu}$ = 3427 m, 1548 s, 1492 m, 1415 s, 1354 s, 1195 m, 921 w, 796 m, 775 m, 565 m cm⁻¹.

X-Ray Crystallography: The single-crystal X-ray data collection of complexes **1** and **3** was performed using a Nonius-Kappa CCD diffractometer, and that of **2** using a Bruker Smart 1000 CCD diffractometer, and graphite-monochromated Mo-K α radiation (λ = 0.71073 Å). Semiempirical absorption corrections were applied. The structures were solved by direct methods and refined by full-matrix least-squares methods on *F*² using the SHELXTL-97 program.^[51] All non-hydrogen atoms were refined using anisotropic displacement parameters. The hydrogen atoms were generated geometrically and treated by a mixture of independent and constrained

refinements. Experimental details of the X-ray data collected for **1**, **2**, and **3** are presented in Table 3. CCDC-224511 to -224513 contain the supplementary crystallographic data for this paper. These data can be obtained free of charge at www.ccdc.cam.ac.uk/conts/retrieving.html [or from the Cambridge Crystallographic Data Centre, 12 Union Road, Cambridge CB2 1EZ, UK; Fax: (internat.) + 44-1223-336-033; E-mail: deposit@ccdc.cam.ac.uk].

Acknowledgments

This work is supported by the National Natural Science Foundation of China (20331010) and the State Key Project of Fundamental Research (G1998061308).

- [1] M. D. Ward, *Science* **2003**, *300*, 1104–1105.
- [2] N. L. Rosi, J. Eckert, M. Eddaoudi, D. T. Vodak, J. Kim, M. O’Keeffe, O. M. Yaghi, *Science* **2003**, *300*, 1127–1129.
- [3] R. Kitaura, S. Kitagawa, Y. Kubota, T. C. Kobayashi, K. Kindo, Y. Mita, A. Matsuo, M. Kobayashi, H. C. Chang, T. C. Ozawa, M. Suzuki, M. Sakata, M. Takata, *Science* **2002**, *298*, 2358–2361.
- [4] S. A. Bourne, J. J. Lu, B. Moulton, M. J. Zaworotko, *Chem. Commun.* **2001**, 861–862.
- [5] Y. Cui, H. L. Ngo, P. S. White, W. B. Lin, *Chem. Commun.* **2003**, 994–995.
- [6] B. Rather, M. J. Zaworotko, *Chem. Commun.* **2003**, 830–831.
- [7] J. Perles, M. Iglesias, C. Ruiz-Valero, N. Snejko, *Chem. Commun.* **2003**, 346–347.
- [8] E. J. Cussen, J. B. Claridge, M. J. Rosseinsky, C. J. Kepert, *J. Am. Chem. Soc.* **2002**, *124*, 9574–9581.
- [9] M. Eddaoudi, H. L. Li, O. M. Yaghi, *J. Am. Chem. Soc.* **2000**, *122*, 1391–1397.
- [10] M. Eddaoudi, J. Kim, M. O’Keeffe, O. M. Yaghi, *J. Am. Chem. Soc.* **2002**, *124*, 376–377.
- [11] L. R. MacGillivray, R. H. Groeneman, J. L. Atwood, *J. Am. Chem. Soc.* **1998**, *120*, 2676–2677.
- [12] Y. C. Liang, R. Cao, W. P. Su, M. C. Hong, W. J. Zhang, *Angew. Chem. Int. Ed.* **2000**, *39*, 3304–3307.
- [13] R. G. Xiong, X. Xue, H. Zhao, X. Z. You, B. F. Abrahams, Z. L. Xue, *Angew. Chem. Int. Ed.* **2002**, *41*, 3800–3803.
- [14] Y. Cui, O. R. Evans, H. L. Ngo, P. S. White, W. B. Lin, *Angew. Chem. Int. Ed.* **2002**, *41*, 1159–1162.
- [15] S. O. H. Gutschke, D. L. Price, A. K. Powell, P. T. Wood, *Angew. Chem. Int. Ed.* **2001**, *40*, 1920–1923.
- [16] Y. H. Wan, L. P. Zhang, L. P. Jin, S. Gao, S. Z. Lu, *Inorg. Chem.* **2003**, *42*, 4985–4994.
- [17] X. J. Zheng, L. P. Jin, S. Z. Lu, *Eur. J. Inorg. Chem.* **2002**, 3356–3363.
- [18] Y. B. Wang, X. J. Zheng, W. J. Zhuang, L. P. Jin, *Eur. J. Inorg. Chem.* **2003**, 1355–1360.
- [19] Y. B. Wang, X. J. Zheng, W. J. Zhuang, L. P. Jin, *Eur. J. Inorg. Chem.* **2003**, 3572–3582.
- [20] L. G. Westin, M. Kritikos, A. Caneschi, *Chem. Commun.* **2003**, 1012–1013.
- [21] R. G. Xiong, X. Z. You, B. F. Abrahams, Z. L. Xue, C. M. Che, *Angew. Chem. Int. Ed.* **2001**, *40*, 4422–4425.
- [22] P. C. R. Soares-Santos, H. I. S. Nogueira, V. Felix, M. G. B. Drew, R. A. Sa Ferreira, L. D. Carlos, T. Trindade, *Chem. Mater.* **2003**, *15*, 100–108.
- [23] O. M. Yaghi, M. O’Keeffe, M. G. Kanatzidis, *J. Solid State Chem.* **2000**, *152*, 1–2.
- [24] S. Nishihara, T. Akutagawa, T. Nakamura, *Inorg. Chem.* **2003**, *42*, 2480–2482.
- [25] R. T. Song, K. M. Kim, Y. S. Sohn, *Inorg. Chem.* **2003**, *42*, 821–826.
- [26] O. M. Yaghi, H. Li, C. Davis, D. Richardson, T. L. Groy, *Acc. Chem. Res.* **1998**, *31*, 474–484.
- [27] S. T. Batten, R. Robson, *Angew. Chem. Int. Ed.* **1998**, *37*, 1460–1494.
- [28] G. Férey, *J. Solid State Chem.* **2000**, *152*, 37–48.
- [29] S. Kitagawa, M. Kondo, *Bull. Chem. Soc. Jpn.* **1998**, *71*, 1739–1753.
- [30] B. L. Chen, M. Eddaoudi, S. T. Hyde, M. O’Keeffe, O. M. Yaghi, *Science* **2001**, *291*, 1021–1023.
- [31] O. M. Yaghi, M. O’Keeffe, N. W. Ockwig, H. K. Chae, M. Eddaoudi, J. Kim, *Nature* **2003**, *423*, 705–714.
- [32] C. Serre, F. Millange, J. Marrot, G. Férey, *Chem. Mater.* **2002**, *14*, 2409–2415.
- [33] A. Dimos, D. Tsaousis, A. Michaelides, S. Skoulika, S. Golhen, L. Ouahab, C. Didierjean, A. Aubry, *Chem. Mater.* **2002**, *14*, 2616–2622.
- [34] L. Pan, K. M. Adams, H. E. Hernandez, X. T. Wang, C. Zheng, Y. Hattori, K. Kaneko, *J. Am. Chem. Soc.* **2003**, *125*, 3062–3067.
- [35] M. Eddaoudi, J. Kim, N. Rosi, D. Vodak, J. Wachter, M. O’Keeffe, O. M. Yaghi, *Science* **2002**, *295*, 469–472.
- [36] R. Cao, D. F. Sun, Y. C. Liang, M. C. Hong, K. Tatsumi, Q. Shi, *Inorg. Chem.* **2002**, *41*, 2087–2094.
- [37] L. Pan, E. B. Woodlock, X. Wang, *Inorg. Chem.* **2000**, *39*, 4174–4178.
- [38] B. Q. Ma, D. S. Zhang, S. Gao, T. Z. Jin, C. H. Yan, G. X. Xu, *Angew. Chem. Int. Ed.* **2000**, *39*, 3644–3646.
- [39] R. Wang, H. Liu, M. D. Carducci, T. Jin, C. Zheng, Z. Zheng, *Inorg. Chem.* **2001**, *40*, 2743–2750.
- [40] K. O. Kongshaug, H. Fjellvag, *Solid State Sci.* **2002**, *4*, 443–447.
- [41] D. W. Min, S. S. Yoon, C. Lee, C. Y. Lee, M. Suh, Y. J. Hwang, W. S. Han, S. W. Lee, *Bull. Korean Chem. Soc.* **2001**, *22*, 531–533.
- [42] J. A. Kaduk, J. A. Hanko, *J. Appl. Crystallogr.* **2001**, *34*, 710–714.
- [43] S. L. Zheng, M. L. Tong, S. D. Tan, Y. Wang, J. X. Shi, Y. X. Tong, H. K. Lee, X. M. Chen, *Organometallics* **2001**, *20*, 5319–5325.
- [44] Y. K. Lee, S. W. Lee, *Bull. Korean Chem. Soc.* **2003**, *24*, 906–910.
- [45] S. W. Lee, H. J. Kim, Y. K. Lee, K. Park, J. H. Son, Y. U. Kwon, *Inorg. Chim. Acta* **2003**, *353*, 151–158.
- [46] K. O. Kongshaug, H. Fjellvag, *Solid State Sci.* **2003**, *5*, 303–310.
- [47] D. W. Min, S. W. Lee, *Bull. Korean Chem. Soc.* **2002**, *23*, 948–952.
- [48] A. Deluzet, W. Maudez, C. Daiguebonne, O. Guillou, *Cryst. Growth Des.* **2003**, *3*, 475–479.
- [49] F. A. A. Paz, J. Klinowski, *Chem. Commun.* **2003**, 1484–1485.
- [50] O. Kahn, *Molecular Magnetism*, VCH Publishers, New York, **1993**.
- [51] G. M. Sheldrick, *SHELXTL-97, Program for the Refinement of Crystal Structures*, University of Göttingen, Germany, **1997**.

Received November 26, 2003

Early View Article

Published Online May 13, 2004